John von Neumann Institute for Computing

Many-Body Correlation Effects in Photoexcited Semiconductor Heterostructures

Torsten Meier, Christian Sieh, Stefan Weiser,
Matthias Reichelt, Christoph Schlichenmaier,
Sven Siggelkow, Peter Thomas, Stephan W. Koch

published in

NIC Symposium 2001, Proceedings,
Horst Rollnik, Dietrich Wolf (Editor),
John von Neumann Institute for Computing, Jülich,
NIC Series, Vol. **9**, ISBN 3-00-009055-X, pp. 315-324, 2002.

http://www.fz-juelich.de/nic-series/volume9

Many-Body Correlation Effects in Photoexcited Semiconductor Heterostructures

Torsten Meier, Christian Sieh, Stefan Weiser, Matthias Reichelt, Christoph Schlichenmaier, Sven Siggelkow, Peter Thomas, and Stephan W. Koch

Department of Physics and Material Sciences Center, Philipps University
Renthof 5, 35032 Marburg, Germany
E-mail: {Torsten.Meier, Christian.Sieh, Stefan.Weiser, Matthias.Reichelt, Christoph.Schlichenmaier, Sven.Siggelkow, Peter.Thomas, Stephan.W.Koch}@physik.uni-marburg.de

A microscopic many-body theory describing the optical properties of semiconductors and semiconductor heterostructures is briefly reviewed. The optical response is described by the Semiconductor Bloch Equations, which include many-body effects arising from the Coulomb interaction among the photoexcited carriers. It is demonstrated that, in particular, many-body correlation contributions beyond the Hartree-Fock level strongly influence the optical response and thus have to be treated properly. The microscopic theory is able to predict and reproduce a number of experimentally observable effects. Many of the numerical solutions could only be obtained by using massively parallel computer programs which were run on the Cray T3E system in Jülich.

1 Introduction

To properly describe the optical properties of semiconductors one has to treat the dynamics of the light field, the material excitations, and their interactions. Since it is known from classical electrodynamics that the electric field couples to the polarization of a medium, the description of the material has to include this polarization as a key quantity[1].

In dipole approximation, the light-matter interaction is proportional to the scalar product of electric field and polarization. For a semiconductor that is excited with optical light fields the induced polarization of the material is due to interband transitions from the valence to the conduction bands. For the linear optical absorption spectrum of an unexcited semiconductor, which consists of completely filled valence and empty conduction bands, it is sufficient to consider only these interband transitions and no further material excitations are required. Already in the linear spectra the Coulomb interaction leads to characteristic signatures. These so called excitonic effects are a consequence of the Coulomb attraction between photoexcited electrons and holes[1].

If the semiconductor is not in the ground state before the photoexcitation, or if the exciting light fields are not in the low-intensity limit, one has to go beyond the linear regime and additional material quantities are required to consistently compute the nonlinear optical response. The Coulomb interaction among the optically excited carriers introduces a many-body problem and thus usually no fully exact treatment of the material response is possible. During the last decade, however, a number of approximation schemes have been developed and applied successfully to different excitation regimes[1–8].

One way to consistently include the Coulomb interaction in a theory for the optical response of semiconductors is to treat the many-body terms on the level of the Hartree-Fock approximation. On this level the dynamic material response is described in terms of

the diagonal and off-diagonal components of the reduced single-particle density matrix. Whereas the latter terms are given by interband transitions which determine the optical polarization the former terms are the carrier occupation probabilities in the different bands. On this level the dynamics of optically induced excitations can be described by coupled equations of motion for the reduced single-particle density matrix. These are well-known as the Hartree-Fock Semiconductor Bloch Equations which include Coulombic effects via bandgap and field renormalization[1,2].

In many-particle physics the term *correlation energy* refers to ground state energy contributions beyond the Hartree-Fock level. Similarly, in semiconductor optics all aspects of the nonlinear optical semiconductor response that cannot be described on the basis of a Hartree-Fock treatment are called *correlation effects*. To theoretically describe such many-body correlations different schemes have been developed.

The second Born approximation[2–5] includes terms which are of second-order in the Coulomb interaction and keeps the reduced single-particle density matrix as the dynamic object. It is applicable to the regime of strong fields and is well suited to describe exciton saturation and excitation-induced dephasing processes due to a plasma of free carriers[7,9,10].

A number of experimentally observable signatures like transitions from excitons to bound biexcitons which are made of two attractively interacting electron-hole pairs, can, however, not be described just on the basis of the reduced single-particle density matrix. One way to treat such processes is to include higher-order, i.e. four- (and more) particle correlations, in the theoretical analysis and to classify the nonlinear optical response in powers of the optical fields[11] using the so-called dynamics-controlled truncation scheme[12,13]. Restricting the analysis to a finite order in the interaction with the optical field closes the many-body hierarchy at a particular level. Since this approach is based on an expansion in powers of the fields, it is limited to the regime of not too strong fields. Nevertheless this scheme has been successfully used to analyze various nonlinear optical experiments performed on semiconductor and semiconductor heterostructures. The results obtained in this context within our project have been described in some reviews[6–8,14] and a number of original publications[15–25].

In Sect. 2 we give a brief review of the microscopic theory that is able to describe the optical response of semiconductors. Some numerical results that are obtained using the dynamics-controlled truncation scheme, which in particular highlight the role of excitonic correlations, are presented in Sect. 3. The paper closes with a short summary in Sect. 4.

2 The Semiconductor Bloch Equations

2.1 Hartree-Fock Approximation

The dynamic optical response of the material is described by the macroscopic optical polarization P. For ordered systems it is convenient to expand the P into a Bloch basis[1]

$$P = \sum_{\mathbf{k},e,h} (d^{eh})^* \; P_{\mathbf{k}}^{eh} + \text{c.c.}\,, \tag{1}$$

where d^{eh} is the electron-hole interband dipole matrix element between conduction band e and valence band h. In terms of electron ($a_k^\dagger$, a_k) and hole ($b_k^\dagger$, b_k) creation and destruction

operators the microscopic polarization $P_{\mathbf{k}}^{eh}$ and the carrier occupation probabilities $f_k^{ee,hh}$ are the diagonal and off-diagonal elements of the reduced single-particle density matrix:

$$\begin{pmatrix} \langle a_k^\dagger\, a_k\rangle & \langle b_{-k}\, a_k\rangle \\ \langle a_k^\dagger\, b_{-k}^\dagger\rangle & \langle b_{-k}^\dagger\, b_{-k}\rangle \end{pmatrix} = \begin{pmatrix} f_k^{ee} & P_k^{eh} \\ (P_k^{eh})^* & f_k^{hh} \end{pmatrix}. \tag{2}$$

The standard many-body Hamiltonian considered in semiconductor optics is[1]

$$H = H_0 + H_C + H_I. \tag{3}$$

Here,

$$H_0 = \sum_{k,e} \varepsilon_k^e a_k^\dagger\, a_k + \sum_{k,h} \varepsilon_k^h b_{-k}^\dagger\, b_{-k} \tag{4}$$

is the single-particle Hamiltonian containing the bandstructure (ε_k^e and ε_k^h),

$$\begin{aligned} H_C = \frac{1}{2} \sum_{k,k',q\neq 0,e,e'} V_q a_{k+q}^\dagger a_{k'-q}^{'\dagger} a_{k'}^{'} a_k + \frac{1}{2} \sum_{k,k',q\neq 0,h,h'} V_q b_{k+q}^\dagger b_{k'-q}^{'\dagger} b_{k'}^{'} b_k \\ - \sum_{k,k',q\neq 0,e,h} V_q a_{k+q}^\dagger b_{k'-q}^{'\dagger} b_{k'}^{'} a_k \end{aligned} \tag{5}$$

describes the Coulomb interaction among the photoexcited carriers, and

$$H_I = -E(t) \sum_{k,e,h} (d^{eh} a_k^\dagger b_{-k}^\dagger + (d^{eh})^* b_{-k} a_k) \tag{6}$$

denotes the dipole interaction with a classical electromagnetic field[1].

The Coulomb interaction, Eq. (5), is given by the sum of three terms describing the repulsion among electrons and holes and the attraction between electrons and holes. V_q is the Fourier transform of the Coulomb interaction potential. The light field, Eq. (6), creates or destroys *pairs* of electrons and holes. In all equations the operators a_k and b_k as well as the corresponding creation operators refer to bands e and h, respectively, and similarly $a_k^{'}$ and $b_k^{'}$ belong to e' and h'.

The Heisenberg equation of motion for P_k^{eh} reads[1]

$$\begin{aligned} i\hbar \frac{\partial}{\partial t} P_k^{eh} = \left[\, P_k^{eh}, H \,\right] = & -\left(\varepsilon_k^e + \varepsilon_k^h\right) P_k^{eh} + \left(d^{eh} - f_k^{ee'} d^{e'h} - d^{eh'} f_k^{h'h}\right) E \\ & + \sum_{q\neq 0} V_q P_{k-q}^{eh} \quad - \sum_{q\neq 0,k'} V_q \left[\left\langle a_k^\dagger a_{k'}^{'\dagger} b_{k+q}^\dagger a_{k'-q}^{'} \right\rangle - \left\langle a_{k+q}^\dagger a_{k'}^{'\dagger} b_k^\dagger a_{k'-q}^{'} \right\rangle \right. \\ & \left. + \left\langle a_{k+q}^\dagger b_{k'+q}^{'\dagger} b_k^\dagger b_{k'}^{'} \right\rangle - \left\langle a_k^\dagger b_{k'+q}^{'\dagger} b_{k-q}^\dagger b_{k'}^{'} \right\rangle \right], \end{aligned} \tag{7}$$

where $e = e'$ and $h = h'$ in the two-band case with only one relevant conduction and valence band. In the more general multiband configuration the primed superscripts correspond to summations over all the relevant bands.

Besides the coupling of the components of the density matrix among themselves (via $H_0 + H_I$) Eq. (7) and the corresponding equations for the carrier occupation probabilities contain terms that couple the two-operator terms to four-operator terms (via H_C). This is the beginning of the well known many-body hierarchy: If one writes equations of motion

for the four-operator expectation values, one obtains a coupling to six-operator terms, and so on. To close the coupled set of equations, one has to truncate this hierarchy at some level in a self consistent fashion.

The dynamical Hartree-Fock approximation uses a decoupling scheme like

$$\left\langle a_k^\dagger \; a_{k'-q}^\dagger \; a_{k-q} \; a_{k'} \right\rangle \simeq \left\langle a_k^\dagger \; a_k \right\rangle \left\langle a_{k-q}^\dagger \; a_{k-q} \right\rangle \; \delta_{k,k'} \; , \tag{8}$$

where no other contribution appears since $q \neq 0$. Applying this procedure to all terms one obtains the well-known Hartree-Fock Semiconductor Bloch Equations. For a two-band system these are given by[1,2]

$$\begin{aligned} \left[i\hbar \frac{\partial}{\partial t} - \epsilon_k^e(t) - \epsilon_k^h(t) \right] P_k^{eh}(t) &= \left[1 - f_k^{ee}(t) - f_k^{hh}(t) \right] \Omega_k(t) \, , \\ \frac{\partial}{\partial t} \; f_k^{aa}(t) &= -\frac{2}{\hbar} \mathrm{Im} \left[\Omega_k(t) (P_k^{eh}(t))^* \right] \; , \end{aligned} \tag{9}$$

where

$$\Omega_k(t) = d^{eh} \; E(t) + \sum_{k' \neq k} V_{k-k'} \; P_{k'}^{eh}(t) \; , \;\; \epsilon_k^a(t) \; = \; \varepsilon_k^a - \sum_{k' \neq k} V_{k-k'} \; f_{k'}^{aa}(t) \tag{10}$$

are the renormalized field and transition energy, respectively. These Hartree-Fock or exchange renormalizations couple all k-states of the semiconductor and furthermore introduce optical nonlinearities in the Hartree-Fock Semiconductor Bloch Equations. The renormalization contributions are no small corrections, with the field renormalization which includes the excitonic effects observable in linear spectra being the leading-order Coulomb effect. The nonlinearities in the Hartree-Fock Semiconductor Bloch Equations, Eq. (9), arise due to phase-space filling (terms proportional to the occupation probabilities times the field Ef), as well as energy and field renormalization. These nonlinearities are a consequence of the Fermionic nature of the electrons and holes (Pauli blocking and Fermionic exchange).

2.2 Dynamics Controlled Truncation

If the analysis of the nonlinear optical response is restricted to a finite order in the interaction with the light field[11] the many-body hierarchy of equations of motion closes at a certain stage[12,13]. Such a procedure establishes a systematic truncation scheme of the Coulombic many-body correlations for purely coherent optical excitation configurations. In the following we present the dynamic equations as obtained in the coherent $\chi^{(3)}$-limit[12,13,26].

In order to be able to distinguish between the Hartree-Fock and the correlation contributions it is convenient to define the correlation function

$$\bar{B}_{k,k',k'',k'''}^{eh'e'h} = \left\langle a_k^\dagger b_{k'}^{'\dagger} a_{k''}^{'\dagger} b_{k'''}^\dagger \right\rangle \; - \; \left\langle a_k^\dagger b_{k'}^\dagger \right\rangle \left\langle a_{k''}^{'\dagger} b_{k'''}^{'\dagger} \right\rangle - \left\langle a_k^\dagger b_{k'''}^{'\dagger} \right\rangle \left\langle a_{k''}^{'\dagger} b_{k'}^\dagger \right\rangle \tag{11}$$

such that the polarization equation in third order can be written as[26]

$$\frac{\partial}{\partial t} P_k^{eh} = \frac{\partial}{\partial t} P_k^{eh}|_{hom} + \sum_{n=1}^{3} \frac{\partial}{\partial t} P_k^{eh}|_{inhom,n} \; , \tag{12}$$

with

$$i\hbar\frac{\partial}{\partial t}P_k^{eh}|_{hom} = -\left(\varepsilon_k^e + \varepsilon_k^h\right)P_k^{eh} + \sum_q V_q P_{k-q}^{eh}\,, \tag{13}$$

$$i\hbar\frac{\partial}{\partial t}P_k^{eh}|_{inhom,1} = \left(d^{eh} - \sum_{e'h'}\left[d^{e'h}(P_k^{eh'})^* P_k^{e'h'} - d^{eh'}(P_k^{e'h})^* P_k^{e'h'}\right]\right)E\,, \tag{14}$$

$$\begin{aligned} i\hbar\frac{\partial}{\partial t}P_k^{eh}|_{inhom,2} = -\sum_{q,e',h'} V_q \Big[& P_k^{eh'}\left(P_k^{e'h'}\right)^* P_{k-q}^{e'h} - P_{k+q}^{eh'}\left(P_{k+q}^{e'h'}\right)^* P_k^{e'h} \\ & + P_{k+q}^{eh'}\left(P_k^{e'h'}\right)^* P_k^{e'h} - P_k^{eh'}\left(P_{k-q}^{e'h'}\right)^* P_{k-q}^{e'h}\Big]\,, \end{aligned} \tag{15}$$

$$\begin{aligned} i\hbar\frac{\partial}{\partial t}P_k^{eh}|_{inhom,3} = \sum_{k',q,e',h'} V_q \left(P_{k'}^{e'h'}\right)^* \Big[& \bar{B}_{k,k',k'-q,k-q}^{eh'e'h} - \bar{B}_{k+q,k',k'-q,k}^{eh'e'h} \\ & + \bar{B}_{k+q,k'+q,k',k}^{eh'e'h} - \bar{B}_{k,k'+q,k',k-q}^{eh'e'h}\Big]\,. \end{aligned} \tag{16}$$

The homogeneous part of Eq. (12) contains the kinetic energies of electrons and holes plus their Coulomb attraction, i.e. the exciton problem, see Eq. (13). The terms denoted with the subscript $inhom$ in Eq. (12) are the different inhomogeneous *driving* terms. The direct coupling to the electromagnetic field is represented by Eq. (14), which includes the linear optical coupling ($d^{eh}E$) and the phase-space filling contributions. Further optical nonlinearities arise in Eq. (12) as a consequence of the many-body Coulomb interaction. The first-order Coulomb contributions are proportional to VPP^*P, see Eq. (15). Those, together with the phase-space filling terms define the Hartree-Fock limit. The *correlation contributions* to the polarization equation, see Eq. (16), consist of four terms of the structure $VP^*\bar{B}$, where $\bar{B}$ is the four-particle correlation function defined in Eq. (11). We thus see that due to the many-body Coulomb interaction the two-particle electron-hole amplitude is coupled to higher-order correlation functions.

The equation for the $\bar{B}$'s can be written as[26]

$$\frac{\partial}{\partial t}\bar{B}_{k,k',k'',k'''}^{eh'e'h} = \frac{\partial}{\partial t}\bar{B}_{k,k',k'',k'''}^{eh'e'h}|_{hom} + \frac{\partial}{\partial t}\bar{B}_{k,k',k'',k'''}^{eh'e'h}|_{inhom}\,, \tag{17}$$

with

$$\begin{aligned} i\hbar\frac{\partial}{\partial t}\bar{B}_{k,k',k'',k'''}^{eh'e'h}|_{hom} = & -\left(\varepsilon_k^e + \varepsilon_{k'}^{h'} + \varepsilon_{k''}^{e'} + \varepsilon_{k'''}^{h}\right)\bar{B}_{k,k',k'',k'''}^{eh'e'h} \\ & + \sum_{q'} V_{q'}\Big[\bar{B}_{k+q',k'+q',k'',k'''}^{eh'e'h} - \bar{B}_{k+q',k',k''-q',k'''}^{eh'e'h} \\ & + \bar{B}_{k+q',k',k'',k'''+q'}^{eh'e'h} + \bar{B}_{k,k'+q',k''+q',k'''}^{eh'e'h} - \bar{B}_{k,k'+q',k'',k'''-q'}^{eh'e'h} + \bar{B}_{k,k',k''+q',k'''+q'}^{eh'e'h}\Big]\,, \end{aligned} \tag{18}$$

$$\begin{aligned} i\hbar\frac{\partial}{\partial t}\bar{B}_{k,k',k'',k'''}^{eh'e'h}|_{inhom} = & -V_{k-k'''}\left(P_{k'''}^{eh} - P_k^{eh}\right)\left(P_{k'}^{e'h'} - P_{k''}^{e'h'}\right) \\ & + V_{k-k'}\left(P_{k'}^{eh'} - P_k^{eh'}\right)\left(P_{k'''}^{e'h} - P_{k''}^{e'h}\right)\,. \end{aligned} \tag{19}$$

Here, the homogeneous part of the equation for $\bar{B}$ is given by Eq. (18) which contains the kinetic energies as well as the four attractive and two repulsive interactions between two electrons and two holes; this defines the *biexciton problem*. The driving terms in Eq. (17)

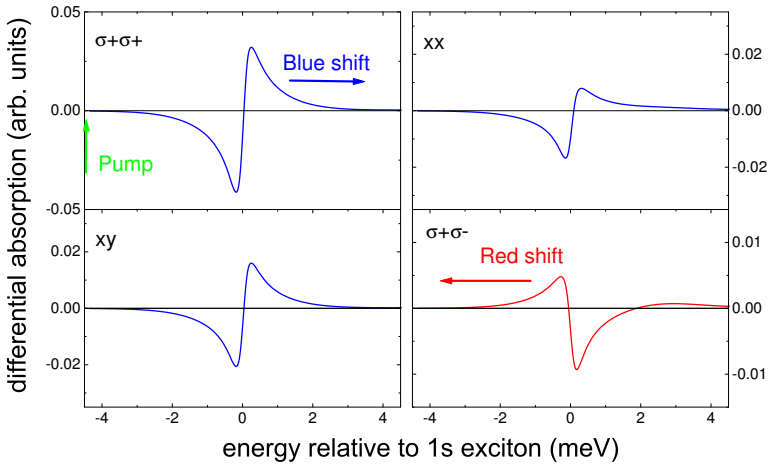

Figure 1. Polarization-dependent differential absorption in optical Stark effect configuration pumping $4.5meV$ below the $1s$ exciton resonance. The origin of the energy scale coincides with the spectral position of the $1s$ exciton (from Ref. [15]).

consist of the Coulomb interaction potential times products of two polarizations, VPP, see Eq. (19).

3 Numerical Results

On the basis of Eqs. (12) and (17) and its extensions accounting for multiple valence bands and higher-order interactions with the field a variety of optical excitation configurations such as pump-probe or four-wave-mixing experiments have been analyzed. In the following we describe three examples where is has been shown that the dynamics of many-body correlations are of particular importance[15, 18, 20].

3.1 Excitonic Optical Stark Effect

A pump-probe experiment is performed using two laser pulses, the pump and the probe. One then monitors the changes of the absorption of the probe pulse induced by the excitation with the pump. This differential absorption $\delta\alpha(\omega)$ is proportional to the Fourier-transform of the pump-induced differential polarization $\delta P(\omega)$[1].

Theoretical results for the light-polarization dependent excitonic optical Stark effect, i.e. the induced spectral changes around the exciton for detuned optical pumping below the resonance, are displayed in Fig. 1. For co-circularly and for linearly polarized pump and probe beams one obtains a spectral blue shift of the exciton reflected in the dispersive-type absorption changes that are positive above and negative below the exciton. This blue shift is the "classical" result well-known from a simple two-level system that is pumped spectrally below its resonance frequency and can simply be understood in terms of level repulsion between the light field and the optical resonance. However, for cross-circularly polarized pulses ($\sigma^+\sigma^-$) the sign of the shift is reversed, i.e. a spectral shift of the exciton

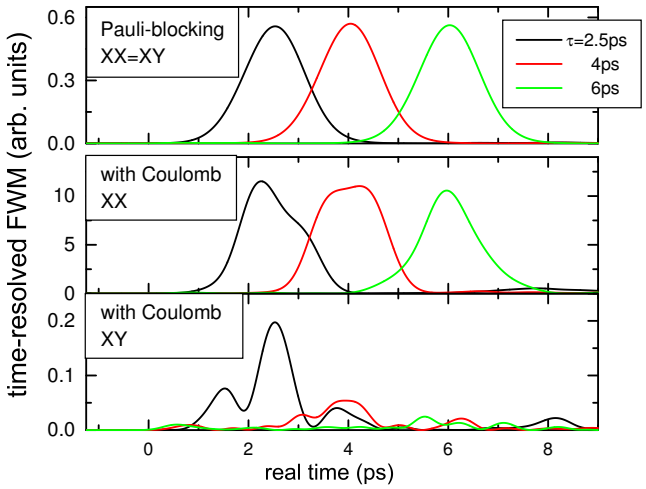

Figure 2. Polarization-dependent time-resolved four-wave-mixing signals for a disordered semiconductor nanostructure using pulse delays $\tau = 2.5$, 4, and $6ps$. The disorder strength is much weaker than the exciton binding energy. For the upper panel many-body correlations are neglected, whereas for the lower panels both disorder and Coulomb correlations have been considered on a microscopic level (from Ref. [20]).

towards the pump (red shift) is found. The calculated polarization-dependent shifts are in agreement with experiments performed on semiconductor quantum wells[15].

For the case of cross-circularly polarized pump and probe pulses it has been shown that the signal is solely induced by many-particle correlations, since the Hartree-Fock contributions vanish as long as only heavy-hole and no light-hole transitions are relevant. This is due to the fact that the two degenerate heavy-hole excitons that can be excited with σ^+ and σ^- polarized light share no common electronic state and are thus uncoupled if many-particle correlations are not taken into account[15,16,19,23]. Whereas the Hartree-Fock contributions which correspond to a blue shift dominate the signal for all other configurations, for $\sigma^+\sigma^-$ one selectively probes only the correlation terms which result in the red shift. The occurrence of this red shift is not directly related to the existence of a bound biexciton that can be excited with $\sigma^+\sigma^-$ polarized pulses. Instead, as shown in Ref.[15] the red shift can be identified to be a genuine consequence of the memory character (non Markovian dynamics) of the many-body correlations dynamics.

3.2 Disorder-Induced Dephasing

A four-wave-mixing experiment is performed using two laser pulses from directions $\mathbf{k}_1$ and $\mathbf{k}_2$ which are temporally delayed by the time delay τ. One then detects the field that is diffracted in the direction $2\mathbf{k}_2 - \mathbf{k}_1$. For optically thin samples this signal is proportional to $|P_{2\mathbf{k}_2-\mathbf{k}_1}(t,\tau)|^2$, see Ref.[1].

In Ref.[20] we have presented numerical solutions of the real-space version of Eqs. (12) and (17) including energetic disorder in the valence and conduction bands. The analysis of disorder effects is important since almost all epitaxy-grown semiconductor heterostructures contain some type of imperfections. For example, the disorder relevant in two-dimensional

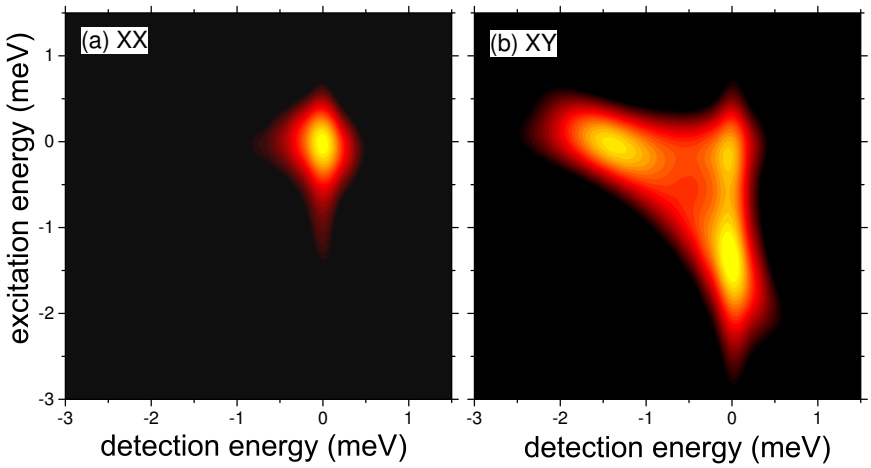

Figure 3. Polarization-dependent contour plots of the coherent excitation spectroscopy scans for linear parallel (a) and perpendicular (b) polarized pulses using a logarithmic scale. The origin of the energy scale coincides with the spectral position of the $1s$ exciton.

quantum wells may come from rough interfaces or may be due to alloy disorder if the well material is a ternary compound made of three types of atoms, like in $(In_xGa_{1-x})As$. To include the disorder we average our numerical solutions over individual disorder realizations until the results converge. This procedure involves a large number of independent calculations which can be very efficiently performed on parallel computers like the Cray T3E.

Due to the disorder-induced inhomogeneous broadening, the time-resolved four-wave-mixing signals for disordered semiconductor nanostructures are emitted as so called photon echoes[1]. This means the signal has its maximum not immediately after the excitation, but that it is peaked at the time delay τ. If correlations are neglected the amplitude of these echoes is independent of the chosen linear polarizations of the laser pulses and of the time delay, upper panel of Fig. 1. The independence of the signal amplitude on τ corresponds to the absence of so called *dephasing* processes, which destroy the phase coherence of the optical polarization.

To be able to describe the experimentally observed polarization dependence of the four-wave-mixing signals many-body correlations are essential. As shown in the lower panels of Fig. 2, with correlations the signals are different for XX and XY excitation configurations. Whereas for XX no obvious dephasing is present, the signal amplitudes are much weaker for XY additionally decrease rapidly with increasing τ. This polarization-dependent decay can only be properly described when both the disorder and the many-body correlations are treated adequately. The estimated decay rates are in good qualitative agreement with experimental results as shown in Ref.[20].

3.3 Coherent Excitation Spectroscopy

Coherent excitation spectroscopy is an example for the so called partially non-degenerate four-wave-mixing. In coherent excitation spectroscopy pulse $\mathbf{k}_1$ is temporally long (spec-

trally narrow), whereas pulse $\mathbf{k}_2$ is short (spectrally broad). Since the long pulse $\mathbf{k}_1$ excites only transitions in a narrow spectral region around its center frequency ω_1, the coherent excitation spectroscopy scans obtained from the coherent signal diffracted in direction $2\mathbf{k}_2 - \mathbf{k}_1$ are ideally suited to investigate coherent couplings among different subsystems and also within disorder broadened lines[18]. The coherent excitation spectroscopy signal is proportional to the Fourier-transform of the four-wave-mixing polarization $|P_{2\mathbf{k}_2-\mathbf{k}_1}(\omega, \omega_1, \tau)|^2$ and depends on both the detection and excitation frequencies, ω and ω_1, respectively.

In Fig. 3 we display the polarization dependence of the coherent excitation spectroscopy scans for linearly polarized pulses. As in Fig. 2 the differences between between XX and XY excitation are solely induced by many-body Coulomb correlations. For XX excitation, Fig. 3(a), one finds only a single peak which occurs at the position of the exciton ($\omega = 0$) when it is resonantly excited by pulse $\mathbf{k}_1$ ($\omega_1 = 0$). For XY, Fig. 3(b), however, three peaks are present. The two additional peaks occur at $\omega \approx -1.5meV$ when $\omega_1 = 0$ and at $\omega = 0$ when $\omega_1 \approx -1.5meV$. $1.5meV$ is just the biexciton binding energy as has been confirmed by additional independently performed calculations. Thus the former one of the two additional peaks is simply due to the exciton-biexciton transition which shows up in four-wave-mixing after the exciton has been excited *resonantly*. The peak obtained for $\omega_1 \approx -1.5meV$, however, results from a exciton-biexciton transition starting from an *off-resonantly* driven exciton transition[27]. More detailed investigations of the correlation signatures contained in the coherent excitation spectroscopy scans including multiple valence bands have recently been performed[27].

4 Summary

A microscopic many-body theory describing the optical and electronic properties of semiconductors and semiconductor heterostructures has been briefly reviewed. The main steps involved in the derivation of the Semiconductor Bloch Equations with many-body correlation contributions beyond the Hartree-Fock level have been discussed. The importance of these correlations for polarization-dependent pump-probe and four-wave-mixing experiments has been demonstrated by showing numerical results for a few selected examples. Many of our results, in particular those on the disorder-induced dephasing and the coherent excitation spectroscopy, could only be obtained using massively parallel computer programs which were run on the Cray T3E system in Jülich. Presently, our grant on this machine allows us to use 27500 KE (Kontingenteinheiten) per month, which corresponds to a monthly usage of 10000 hours of computer time on a single processor.

Acknowledgments

This work is supported by the Deutsche Forschungsgemeinschaft (DFG) through the Leibniz prize, the Schwerpunkt Quantenkohärenz, and the project No. KO816/8-1. We wish to thank the John von Neumann - Institut für Computing (NIC), Forschungszentrum Jülich, Germany, for grants for extended CPU time on their supercomputer systems.

References

1. H. Haug and S. W. Koch, "Quantum Theory of the Optical and Electronic Properties of Semiconductors", 3rd ed., World Scientific Publ., Singapore (1994).
2. M. Lindberg and S.W. Koch, Phys. Rev. B **38**, 3342 (1988).
3. R. Binder and S.W. Koch, Prog. Quant. Electron. **19**, 307 (1995).
4. W. Schäfer, Journ. Opt. Soc. Am. B **13**, 1291 (1996).
5. F. Jahnke, M. Kira, and S.W. Koch, Z. Physik B **104**, 559 (1997).
6. S.W. Koch, T. Meier, F. Jahnke, and P. Thomas, Appl. Phys. A **71**, 511 (2000).
7. T. Meier and S.W. Koch, in *Semiconductors and Semimetals* Vol. 67, "Ultrafast Physical Processes in Semiconductors", pp. 231-313, Academic Press (2001).
8. S.W. Koch, M. Kira, and T. Meier, J. of Optics B **3**, R29-R45 (2001) .
9. H. Wang, K. Ferrio, D.G. Steel, Y.Z. Hu, R. Binder, and S.W. Koch, Phys. Rev. Lett. **71**, 1261 (1993).
10. F. Jahnke, M. Kira, S.W. Koch, G. Khitrova, E.K. Lindmark, T.R. Nelson, D.V. Wick, J.D. Berger, O. Lyngnes, H.M. Gibbs, and K. Tai, Phys. Rev. Lett. **77**, 5257 (1996).
11. N. Bloembergen, Nonlinear Optics, Benjamin Inc., New York (1965).
12. M. Lindberg, Y.Z. Hu, R. Binder, and S. W. Koch, Phys. Rev. B **50**, 18060 (1994).
13. V.M. Axt and A. Stahl, Z. Phys. B **93**, 195 and 205 (1994).
14. T. Meier, Habilitation-Thesis *Theory of Electric Field Effects and Many-Body Correlations in Semiconductor Optics*, Department of Physics, Philipps-University Marburg, 2000.
15. C. Sieh, T. Meier, F. Jahnke, A. Knorr, S.W. Koch, P. Brick, M. Hübner, C. Ell, J. Prineas, G. Khitrova, and H.M. Gibbs, Phys. Rev. Lett. **82**, 3112 (1999).
16. C. Sieh, T. Meier, A. Knorr, F. Jahnke, P. Thomas, and S.W. Koch, Europ. Phys. J. B **11**, 407 (1999).
17. T. Meier and S.W. Koch, Phys. Rev. B **59**, 13202 (1999).
18. A. Euteneuer, E. Finger, M. Hofmann, W. Stolz, T. Meier, P. Thomas, S.W. Koch, W.W. Rühle, R. Hey, and K. Ploog, Phys. Rev. Lett. **83**, 2073 (1999).
19. S.W. Koch, C. Sieh, T. Meier, F. Jahnke, A. Knorr, P. Brick, M. Hübner, C. Ell, J. Prineas, G. Khitrova, and H.M. Gibbs, J. of Lumin. **83/84**, 1 (1999).
20. S. Weiser, T. Meier, J. Möbius, A. Euteneuer, E.J. Mayer, W. Stolz, M. Hofmann, W.W. Rühle, P. Thomas, and S.W. Koch, Phys. Rev. B **61**, 13088 (2000).
21. T. Meier, S.W. Koch, P. Brick, C. Ell, G. Khitrova, and H.M. Gibbs, Phys. Rev. B **62**, 4218 (2000).
22. T. Meier, S.W. Koch, M. Phillips, and H. Wang, Phys. Rev. B **62**, 12605 (2000).
23. P. Brick, C. Ell, G. Khitrova, H.M. Gibbs, T. Meier, C. Sieh, and S.W. Koch, Phys. Rev. B **64**, 075323-1 (2001).
24. W. Langbein, T. Meier, S.W. Koch, and J.M. Hvam, J. Opt. Soc. Am. B **18**, 1318 (2001).
25. H.P. Wagner, H.-P. Tranitz, M. Reichelt, T. Meier, and S.W. Koch, Phys. Rev. B **64** 233303 (2001).
26. W. Schäfer, D. S. Kim, J. Shah, T. C. Damen, J. E. Cunningham, K. W. Goosen, L. N. Pfeiffer, and K. Köhler, Phys. Rev. B **53**, 16429 (1996).
27. E. Finger, S.P. Kraft, M. Hofmann, T. Meier, S.W. Koch, W. Stolz, and W.W. Rühle, submitted to Phys. Rev. B.